Available online at www.sciencedirect.com
ScienceDirect
Catalysis Today 119 (2007) 100–105
CATALYSIS TODAY
www.elsevier.com/locate/cattod

# An in situ study of the $NO + H_2 + O_2$ reaction on $Pd/LaCoO_3$ based catalysts

I. Twagirashema [a], M. Engelmann-Pirez [a], M. Frere [a], L. Burylo [b], L. Gengembre [a], C. Dujardin [a,*], P. Granger [a]

[a] *Laboratoire de Catalyse de Lille, UMR CNRS 8010, Bât C3, Université des Sciences et Technologies de Lille, 59655 Villeneuve D'ascq Cedex, France*
[b] *Laboratoire de Cristallochimie et Physico-Chimie du Solide, UMR CNRS 8012, Bât C7, Université des Sciences et Technologies de Lille, 59655 Villeneuve D'ascq Cedex, France*

---

**Abstract**

In situ X-ray diffraction (XRD) and quasi in situ X-ray photoelectron spectroscopy (XPS) measurements were complementary used to investigate structural and surface modifications of a palladium-supported on $LaCoO_3$ perovskite catalyst under various controlled atmospheres, particularly during the reduction of NO by hydrogen under lean conditions, in the presence of a large excess of oxygen.

An extensive reduction of the perovskite was evidenced during the pre-activation thermal treatment of the palladium-supported catalyst under hydrogen at 773 K leading to the formation of Pd particles in contact with $Co^0$ and $La_2O_3$. In the presence of an excess of oxygen, the catalyst structure changes during the reaction. The reduced solid is progressively transformed into $LaCoO_3$ in the range of 873–1173 K. However, such a bulk transformation probably occurs at lower temperatures at the surface of the solid according to XPS analyses. At the same time, the binding energy (BE) level of the Pd $3d_{5/2}$ photopeak increases up to 337.5 eV which reveals the stabilisation of oxidic palladium species in a different chemical environment than that corresponding to PdO. Such changes induced different catalytic properties of the catalyst during the reduction of NO by $H_2$.

*Keywords:* NO; XRD; XPS; Perovskite; Hydrogen; Cobalt; Palladium

---

## 1. Introduction

Several perovskite-type solids have been recognized for their oxidation/reduction properties with many potential applications in environmental catalysis, for example to control automotive exhaust emissions such as nitrogen oxide ($NO_x$), carbon monoxide (CO), and unburned hydrocarbons [1–4]. Moreover perovskite-type oxides have been found to display interesting catalytic properties and a high thermal stability [5,6]. In the case of stationary sources, the catalyst should be active at low temperature and in the presence of an excess of oxygen. Recent investigations have shown that noble metals-supported perovskite catalysts could be potentially interesting for $NO_x$ reduction for mobile and stationary sources running under lean conditions [4,7], particularly $Pd/LaCoO_3$ [7]. The catalytic properties of palladium for $NO_x$ reduction are quite sensitive to the nature of the support and to the pre-activation thermal treatment. However the perovskite structure is known to be sensitive to reductive treatment [8]. The transformation of $LaCoO_3$ into $Co^0$–$La_2O_3$ is reported to occur at 873 K from in situ temperature programmed XRD experiments [7,9]. By contrast, the perovskite can self-restructure in an oxidizing environment [10,11]. On modified perovskite materials after palladium addition, oxidic palladium species subsequently formed can diffuse and partially substitute Co in B-sites of the perovskite structure [12]. Such changes may originate significant modifications in the catalytic properties.

In order to elucidate the functioning mode of the catalyst, spectroscopic measurements were performed under controlled atmospheres. The pre-activation thermal treatment before reaction drastically modifies the catalytic properties of Pd due to structural changes of the perovskite. The consequences

---

* Corresponding author. Tel.: +33 3 20 43 45 27; fax: +33 3 20 43 65 61.
*E-mail address:* christophe.dujardin@univ-lille1.fr (C. Dujardin).

0920-5861/$ – see front matter © 2006 Elsevier B.V. All rights reserved.
doi:10.1016/j.cattod.2006.08.013

of the preactivation have been examined. Bulk and surface modifications of the solid have been tentatively related to changes in the catalytic behaviour.

## 2. Experimental

### 2.1. Catalyst preparation

$LaCoO_3$ was prepared according to a citrate route [13] using aqueous solutions of $La(NO_3)_3 \cdot 6H_2O$ and $Co(NO_3)_2 \cdot 6H_2O$ with a molar citric acid/(La + Co) ratio of 1. The solid was obtained after evaporation, drying overnight at 353 K and subsequent calcination in flowing air at 873 K for 5 h. Palladium (1 wt.%) was loaded by impregnation of the perovskite with a solution of $Pd(NO_3)_2 \cdot 2H_2O$. The catalyst was then calcined at 673 K during 4 h.

### 2.2. Catalyst characterization

In situ X-ray diffraction (XRD) profiles were recorded using a Bruker D8 $\theta/2\theta$ diffractometer equipped with a Cu Kα ($\lambda = 0.154$ nm) radiation. The sample was in situ reduced under a flow of $H_2$ at 773 K overnight. The reaction mixture (0.15% NO, 0.5% $H_2$, 3% $O_2$, He) was introduced over the catalyst in the XRD chamber at 298 K and the temperature was raised until the desired temperature (3 K/min) with a plateau of 1 h for ageing and 1 h for data acquisition.

XPS experiments were performed using a Vacuum Generators Escalab 220XL spectrometer. A monochromatized aluminium source was used for excitation. Binding energy (BE) values were referenced to the binding energy of La $3d_{5/2}$ (833.7 eV). The pre-activation step and the reaction were performed at atmospheric pressure in a catalytic chamber coupled to the XPS apparatus and the sample was then transferred in the analysis chamber under ultra high vacuum ($\sim 10^{-10}$ Torr) for XPS analysis. Before the reaction, Pd/$LaCoO_3$ samples were activated in $H_2$ by increasing the temperature until 773 K (3 K/min, no plateau), cooled down at room temperature and then treated under the reaction mixture (20 mL/min) 0.15% NO, 0.5% $H_2$, 3% $O_2$ in Helium at a given temperature during 30 min or 2 h. After XPS analysis, the catalyst was transferred in the catalysis chamber for the subsequent temperature in the reaction mixture. In order to quantify the amount of cobalt in different chemical environments, we have used a mixed Gaussian/Lorentzian peak fit keeping binding energies and half-widths (FWHM ± 0.1 eV) constant for all decompositions.

### 2.3. Ex situ catalytic testing

Catalytic measurements were carried out in a fixed bed flow reactor in temperature-programmed conditions between 298 and 773 K (heating rate of 2 K/min, space velocity of 4000 $h^{-1}$). The effluent were analysed with a Shimadzu GC14A gas chromatograph equipped with a thermal conductivity detector. The overall conversion of NO ($\tau_{NO}$) and of $H_2$ ($\tau_{H_2}$) related to the reduction of NO, were calculated according to Eqs. (1) and (2), $\tau_{N_2}$ and $\tau_{N_2O}$ being, respectively, the conversion of NO into nitrogen and nitrous oxide. $n_i^0$ was the inlet amount of the reactant $i$ whereas $n_{N_2}$ and $n_{N_2O}$ were the amounts of $N_2$ and $N_2O$ produced, respectively, at a given time. $p_i^0$ was the inlet partial pressure of the reactant $i$:

$$\tau_{NO} = \frac{2(n_{N_2} + n_{N_2O})}{n_{NO}^0} = \tau_{N_2} + \tau_{N_2O}, \tag{1}$$

$$\tau_{H_2} = \frac{2n_{N_2} + n_{N_2O}}{n_{H_2}^0} = \left(\tau_{N_2} + \frac{\tau_{N_2O}}{2}\right)\frac{p_{NO}^0}{p_{H_2}^0} \tag{2}$$

## 3. Results and discussion

### 3.1. Temperature programmed NO + $H_2$ reaction in the presence of oxygen on pre-reduced Pd/$LaCoO_3$ in $H_2$ at 773 K

As previously mentioned in the experimental section, the NO + $H_2$ reaction is usually described by a two-step reaction with the intermediate formation of $N_2O$:

$$2NO + 2H_2 \rightarrow N_2 + 2H_2O \tag{3}$$

$$2NO + H_2 \rightarrow N_2O + H_2O \tag{4}$$

$$N_2O + H_2 \rightarrow N_2 + H_2O \tag{5}$$

Temperature programmed conversion and selectivity curves are reported in Fig. 1A and B, respectively. As illustrated, two ranges of NO conversion are distinguishable. Below 473 K, the NO + $H_2$ and $H_2 + O_2$ reactions compete, this competition being in favour of the former reaction. A maximum of NO conversion arises near 410 K which coincides with a selectivity value towards the formation of $N_2O$ ($S_{N_2O}$) of approximately 40%. Above that temperature, the conversion sharply drops and then stabilises near 23% in the temperature range 423–773 K. Surprisingly the selectivity ($S_{N_2O}$) remains unchanged, according to the margin of error, whereas a loss of conversion should be accompanied with an increase in the formation of $N_2O$ from a kinetic viewpoint. Consequently such observations probably underline surface modifications in the course of the reaction according to previous investigations performed in our laboratory on pre-reduced $LaCoO_3$-only catalysts. In the present study, Pd addition sharply enhances the activity in the conversion of NO. The two ranges of conversion observed could be explained by different reaction pathways earlier suggested in the literature [14]. The direct reaction of NO by $H_2$ catalysed on metallic palladium particles could be favoured at low temperature, whereas in situ generated $NO_2$ could react with $H_2$ at high temperature mainly on oxidic noble metal species [15,16]. Previous experiments on $LaCoO_3$ reduced into $Co^0$/$La_2O_3$ show that under running conditions, a reconstruction of the rhomboedral structure of $LaCoO_3$ on pre-reduced samples may occur below 773 K [10]. Such modifications could involve palladium species and then explain changes in its intrinsic catalytic properties.

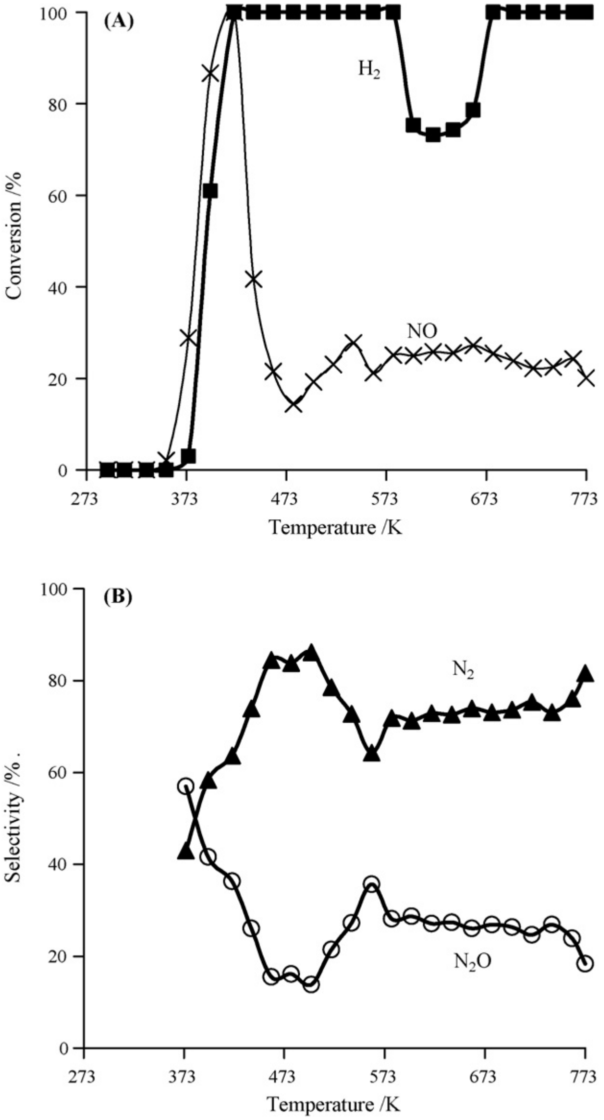

Fig. 1. Temperature-programmed profiles of the overall conversion of NO and $H_2$ (A) and of the selectivity (B) of 1 wt.% Pd–$LaCoO_3$ pre-reduced in $H_2$ at 773 K (reaction mixture 0.15% NO + 0.5% $H_2$ + 3% $O_2$—space velocity 4000 $h^{-1}$).

### 3.2. In situ physico-chemical characterisation of the catalyst during the NO + $H_2$ reaction in the presence of oxygen

#### 3.2.1. Pre-activation thermal treatment in $H_2$

Before reaction, the calcined catalyst was treated under hydrogen at 773 K in order to reduce the palladium particles dispersed on the support. XRD analysis shows that the reductive thermal treatment induces strong structural modifications, the initial rhomboedral structure of the perovskite (Fig. 2A, spectrum a) being transformed into $Co^0$ particles and $La_2O_3$ as illustrated in Fig. 2A (spectrum b). Such transformations are well in agreement with earlier results [10].

After in situ reduction, the examination of Co 2p photopeak shows that the reduction of Co(III) species into $Co^0$ species is not complete since part of the cobalt remains stabilised as $Co^{2+}$ (Table 1) contrarily to XRD observations which suggest a complete reduction. This observation can be explained by the difference between both reduction procedures. During XRD measurements, the plateau under hydrogen at 773 K was maintained overnight whereas during XPS measurements, the reduction of the catalyst was stopped when the temperature reached 773 K. XPS analysis (Fig. 3A) shows a complete reduction of $Pd^{2+}$ entities into $Pd^0$ after $H_2$ exposure at 773 K with a shift of the B.E of the Pd $3d_{5/2}$ photopeak from 336.2 to 335.1 eV [17,18].

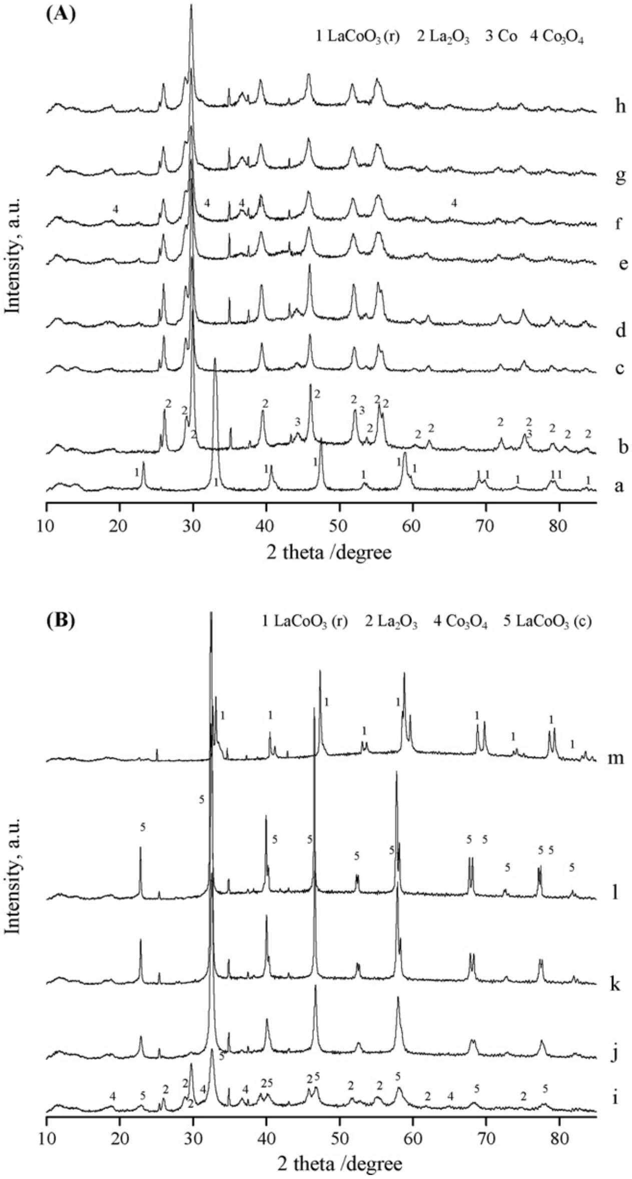

Fig. 2. In situ XRD patterns recorded on 1 wt.% Pd–$LaCoO_3$, after reduction in $H_2$ at 773 K and in the course of the reaction under 0.15% NO + 0.5% $H_2$ + 3% $O_2$ with increasing temperature. (A): (a) calcined 1 wt.% Pd–$LaCoO_3$, (b) after reduction at 773 K, and in the course of the reaction at (c) 298 K, (d) 373 K, (e) 473 K, (f) 573 K, (g) 673 K, (h) 773 K, (B): (i) 873 K, (j) 973 K, (k) 1073 K, (l) 1173 K, and (m) after cooling down to 298 K.

#### 3.2.2. Structural and surface modifications during the NO + $H_2$ + $O_2$ reaction

XRD diffractograms recorded in the course of the reaction are collected in Fig. 2A and B. After exposure at room temperature, the XRD pattern still exhibits the presence of

Table 1
Semi-quantitative analysis from XPS measurements of 1 wt.% Pd–$LaCoO_3$ during the activation, reduction and after reaction under 0.15% NO + 0.5% $H_2$ + 3% $O_2$ at various temperatures

| Analysed step | Binding energy (eV) | | | Atomic quantification of Co | | | Atomic ratio | |
|---|---|---|---|---|---|---|---|---|
| | Co 2p | N 1s | Pd $3d_{5/2}$ | % $Co^{3+}$ | % $Co^{2+}$ | % $Co^0$ | Co/La | Pd/La |
| Fresh | 779.7 | – | 336.2 | 100 | – | – | 0.47 | 0.025 |
| Reduction 773 K | 777.8<br>780 | – | 335.1 | – | 39 | 61 | 0.52 | 0.023 |
| Reaction 298 K, 30 min | 780.1 | 403.4 | 335.3 | – | 100 | – | 0.49 | 0.017 |
| Reaction 473 K, 30 min | 779.8 | 403.2<br>407 | 335.2 | 51 | 49 | – | 0.54 | 0.014 |
| Reaction 573 K, 30 min | 780 | 403.3<br>407 | 335.2<br>336.2<br>337.5 | 100 | – | – | 0.44 | 0.012 |
| Reaction 573 K, 2 h | 779.7 | 403.5<br>407.2 | 335.2<br>336.2<br>337.5 | 100 | – | – | 0.36 | 0.011 |
| Reaction 773 K, 30 min | 780.3 | – | 336.2<br>337.5 | 100 | – | – | 0.50 | 0.014 |
| Reaction 773 K, 2 h | 780 | – | 336.2<br>337.5 | 100 | – | – | 0.44 | 0.010 |

crystalline $La_2O_3$ but the peak-width broadens and its intensity progressively decreases indicating the growth of an amorphous phase. X-ray lines assigned to cobalt metallic particles progressively disappear in the low temperature range and an intermediate $Co_3O_4$ phase is detected between 573 and 873 K (Fig. 2A and B) which disappears with a rise in temperature. It is also worthwhile to note that no bulk palladium species are observable particularly at high temperature where sintering reactions usually take place. Such observations suggest that palladium entities preserve a high degree of dispersion. In fact, structural changes are mainly observed above 773 K with the appearance of additional X-ray lines assigned to the cubic structure of $LaCoO_3$. After cooling down at room temperature, the rhomboedral structure of $LaCoO_3$ is stabilised. As illustrated in this figure, significant structural changes mainly occur at high temperature with the reconstruction of the perovskite. However previous investigations have shown that bulk transformations may be initiated at the surface at lower temperatures [10].

Additional XPS measurements provide interesting spectral features regarding surface changes during the reaction. A particular attention has been paid towards the Pd 3d and the Co 2p photopeaks. Spectral features related to Co are summarised in Table 1. After exposure to the reaction mixture, the surface oxidation of cobalt starts at room temperature and is complete at 573 K. Co 2p photopeaks (not shown) were decomposed according to the calculation routine described in the experimental section, in order to quantify the fraction of cobalt stabilised in various oxidation states. As indicated, surface oxidation starts at room temperature with the complete disappearance of $Co^0$ converted into $Co^{2+}$ species. A subsequent increase in temperature leads to a more extensive oxidation with the formation of $Co^{3+}$ entities. At 473 K, the surface stoichiometry between different cobalt species tends towards the theoretical one characterising $Co_3O_4$ evidenced from XRD measurements. Above 573 K, cobalt is completely oxidised into Co(III) species which indicates that cobalt species are stabilised in a different chemical environment than $Co_3O_4$. Both observations emphasize the fact that the self-reconstruction of the perovskite may occur at a significantly lower temperature than that observed during XRD measurements.

At the same time, interesting information arise from the oxidation state of palladium during the reaction under lean conditions. Pd 3d photopeaks recorded after exposure to the reaction mixture at various temperatures between 298 and 773 K are reported in Fig. 3A. As observed, the palladium preserves its metallic character below 473 K under reaction conditions (BE of 335.1 eV). On the other hand, the shape of photopeak of Pd $3d_{5/2}$ drastically changes after exposure at 573 K. The binding energy of the photopeak shifts toward higher energies indicating an oxidation of metallic palladium atoms.

The broad spectrum recorded at 573 K in Fig. 3A highlights the occurrence of various oxidic palladium species with an apparent maximum at 337.5 eV and a shoulder at 336.2 eV which corresponds to the usual binding energy values for $Pd^{2+}$. On the other hand, the assignment of the contribution located at higher binding energy is controversial. The development of the photopeak at 337.5 eV is clear after 2 h ageing under reaction conditions at 773 K. Such an apparent high binding energy value can be assigned either to the segregation of $Pd^{2+}$ and $Pd^{4+}$ species or to palladium species exhibiting an intermediate oxidation state. In fact, binding energy of Pd $3d_{5/2}$ is usually reported at 336.8 eV in PdO [19] and 338.3 eV in $PdO_2$ or deficiently coordinated (ionic) $Pd^{2+}$ species [20]. Another interesting result which can be linked to the oxidation state of

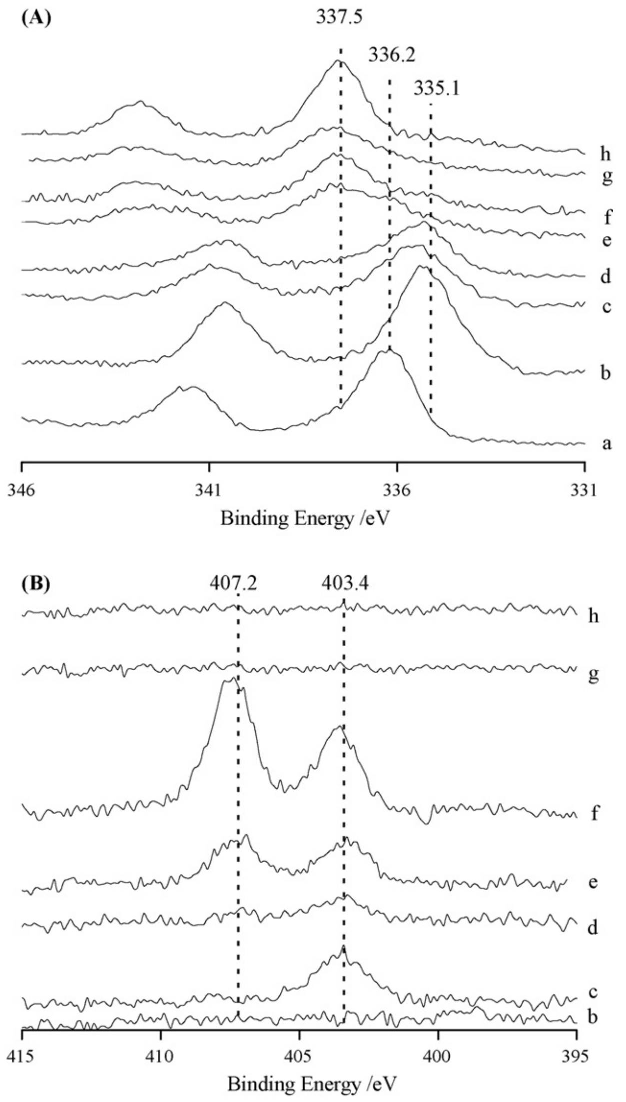

Fig. 3. Pd $3d_{5/2}$ and Pd $3d_{3/2}$ photopeaks (A) and N 1s photopeaks (B) recorded on 1 wt.% Pd–$LaCoO_3$ during XPS analysis: (a) ex situ calcined catalyst, (b) after reduction in $H_2$ at 773 K; after reaction within the following conditions 0.15% NO + 0.5% $H_2$ + 3% $O_2$ (c) at 298 K for 30 min, (d) at 473 K for 30 min, (e) at 573 K for 30 min, (f) at 573 K for 2 h, (g) at 773 K for 30 min and (h) at 773 K for 2 h.

palladium is the rejuvenation of the perovskite evidenced at high temperature from XRD measurements which starts at a lower temperature around 573 K as suggested by XPS observations. Previous studies report the formation of the perovskite in oxidising atmosphere [21] or a self-regeneration of the perovskite during the reaction under lean conditions [11]. In particular, Uenishi et al. [11] suggest the formation of $LaFe_{0.95}Pd_{0.05}O_3$ with part of the palladium inside the framework of the perovskite occupying the B-site. According to Zhou et al. [22], a partial insertion of Pd may lead to a lower overall activity of the catalyst in comparison with palladium-supported perovskite catalyst.

The development of the highest binding energy contribution near 337.5 eV in Fig. 3A with intermediate values between those usually reported for $Pd^{4+}$ in $PdO_2$ and $Pd^{2+}$ in PdO is well in agreement with earlier investigations which evidenced a partial substitution of palladium in the octahedral B-sites of the perovskite. Of course, no final conclusion regarding the location of Pd can be drawn. However the constant decrease of the atomic Pd/La ratio in the course of the reaction is an additional argument which may indicate a partial redistribution of palladium in B-sites of the perovskite structure.

The examination of the photopeak N 1s in Fig. 3B shows that the N-containing species strongly interact with the catalyst. Two contributions arise at 403.4 and 407.2 eV which have been assigned to, respectively, nitrite and nitrate species interacting with either palladium centers or the support material [17]. Above 573 K (see spectra g and h), no signal is observed indicating the desorption/decomposition of those species. This result seems to be well in argument with previous statements. Below 573 K, the palladium is predominantly stabilised into metallic particles which could be essential for catalysing the NO+$H_2$ reaction. XPS measurements performed under ultra high vacuum mainly characterised strongly adsorbed nitrate and nitrite species which could be chemisorbed on $Pd^0$ sites further inhibiting the reaction. However the loss of activity in the conversion of NO above 410 K may be explained differently mainly by a partial oxidation of palladium into PdO as illustrated in Fig. 3A. The competition between the NO + $H_2$ and $H_2$ + $O_2$ reactions becomes in favour of the latter reaction according to the formation of PdO. The residual activity in the NO conversion at high temperature may be questionable. In accordance with the above-mentioned statements, the conversion of NO should strongly attenuate with a rise in temperature. In fact the residual conversion could be explained by a compensation effect involving the development of well-dispersed palladium entities in strong interaction with the perovskite exhibiting a better intrinsic activity towards the NO + $H_2$ reaction.

## 4. Conclusions

Tentative correlations between catalytic and spectroscopic features have been achieved during the reduction of NO by $H_2$ in the presence of an excess of oxygen on pre-reduced Pd/$LaCoO_3$. According to this thermal treatment, an extensive reduction leads to the formation of $Pd^0$ and $Co^0$ particles in interaction with $La_2O_3$. Surface modifications significantly occur at 573 K in the course of the reaction related to the segregation of oxidic palladium species and the reconstruction of the perovskite according to XPS measurements. Such surface changes may explain the residual NO conversion mainly into nitrogen at high temperature.

## References

[1] R.J.H. Voorhoeve, J.P. Remelka, L.E. Trimble, The Catalytic Chemistry of Nitrogen Oxides, Plenum Press, New York, 1975, p. 215.
[2] L.G. Tejuca, J.L.G. Fierro, Properties and Applications of Perovskite-type Oxides, Marcel Dekker Inc., New York, 1993, p. 271.
[3] R.M. Heck, R.J. Farrauto, Catalytic Air Pollution Control: Commercial Technology, Van Nostrand Reinhold, New York, 1995, p. 95.
[4] C.N. Costa, V.N. Stathopoulos, V.C. Belessi, A.M. Efstathiou, J. Catal. 197 (2001) 350.

[5] P. Ciambelli, S. Cimino, S. De Rossi, L. Lisi, G. Minelli, P. Porta, G. Russo, Appl. Catal. B 29 (2001) 239.

[6] R. Leanza, I. Rossetti, L. Fabbrini, C. Oliva, L. Forni, Appl. Catal. B 28 (2000) 55.

[7] M. Engelmann-Pirez, P. Granger, L. Leclercq, G. Leclercq, Topics Catal. 30/31 (2004) 59.

[8] T. Nakamura, G. Petzow, L.J. Gauckler, Mater. Res. Bull. 14 (1979) 649.

[9] F.M. Martinez-Ortega, C. Batiot-Dupeyrat, G. Valderrama, J.M. Tatibouet, C.R. Acad, Sci. Paris Série IIc: Chimie/Chem. 4 (2001) 49.

[10] I. Twagirashema, M. Frere, L. Gengembre, C. Dujardin, P. Granger, Topics in Catalysis, in press.

[11] M. Uenishi, M. Taniguchi, H. Tanaka, M. Kimura, Y. Nishihata, J. Mizuki, T. Kobayashi, Appl. Catal. B 57 (2005) 267.

[12] Y. Nishihata, J. Mizuki, H. Tanaka, M. Uenichi, M. Kimura, J. Phys. Chem. Sol. 66 (2000) 274.

[13] H. Taguchi, S.I. Matsu-ura, M. Nagao, T. Choso, K. Kabata, J. Solid State Chem. 129 (1997) 60.

[14] A. Veda, T. Nakao, M. Azuma, T. Kobayashi, Catal. Today 45 (1998) 135.

[15] R. Burch, M.D. Coleman, Appl. Catal. B 23 (1999) 115.

[16] R. Burch, P.K. Laader, N.A. Cruise, Appl. Catal. A 147 (1996) 375.

[17] D. Briggs, M.P. Seah, Practical Surface Analysis, 2nd ed., John Wiley, Chichester, 1993.

[18] J.F. Moulder, W.F. Stickle, P.E. Sobol, K.D. Bomden, Handbook of X-ray Photoelectron Spectroscopy, Perkin-Elmer Physical Electronic Division, Eden Prairil, MN, 1992.

[19] M. Brun, A. Berthet, J.C. Bertolini, J. Elect. Spectr. Related Phenom. 104 (1999) 55.

[20] K. Otto, L.P. Haack, J.E. deVries, Appl. Catal. B 1 (1992) 1.

[21] J.N. Nudel, B.S. Umansky, E.A. Lombardo, Appl. Catal. 31 (2) (1987) 275.

[22] K. Zhou, H. Chen, Q. Tian, Z. Hao, D. Shen, X. Xu, J. Mol. Catal. A: Chem. 189 (2002) 225.